Reduced Copper Diffusion in Layered Silicate/Fluorinated Polyimide (6FDA-ODA) Nanocomposites

Liang-You Jiang, Kung-Hwa Wei

Department of Materials Science and Engineering, National Chiao Tung University, Hsinchu, Taiwan 30049, ROC

Received 20 December 2002; accepted 31 October 2003

ABSTRACT: The copper diffusion barrier properties of layered silicate/fluorinated polyimide nanocomposites were analyzed by transmission electron microscopy (TEM) and secondary ion mass spectrometry (SIMS). It was found that the particles of copper are effectively retarded from penetrating into the polyimide matrix by layered silicates. The diffusion coefficients of layered silicate/polyimide nanocomposites are lower than that of the pure polyimide. © 2004 Wiley Periodicals, Inc. J Appl Polym Sci 92: 1422–1425, 2004

Key words: copper diffusion; layered silicates; fluorinated polyimide; nanocomposites

INTRODUCTION

High-performance ultra-large-scale integration (ULSI) and giga-scale integration (GSI) devices require materials with low resistivity for the interconnect and low dielectric constant for the interlayer insulator in order to reduce the resistance-capacitance delay. Low bulk resistivity (≥1.67 μΩ cm) copper (Cu) and low dielectric coefficient (≤2.8) fluorinated polyimide (PI) are, therefore, suitable choices for forming multilayered structures in these devices. At the Cu/PI interface, however, Cu tends to diffuse into the polyimide, causing leakage currents[1–3] and device degradation. Hence, several studies on potential barrier layers have been undertaken. One approach involves metal barrier layers such as Ta, Ti, Al, Cr, Ni, W, or various alloys of these metals.[2–5] The second approach adopts organic materials as barrier layers, such as poly(arylene ether benzimidazole) (PAEBI) or others.[3,6,7] The third approach consists of O_2 and N_2 plasma pretreatment of the polyimide surface.[1,8] In this article, an integral approach is taken by combining the barrier material into the polyimide layer, that is, the nanocomposite layer. To our knowledge, this is the first time nanocomposite layers have been used for this purpose.

Layered silicate/polyimide nanocomposites have attracted a great deal of interest owing to substantial improvement over the pristine state in their thermal, mechanical, and barrier properties with the incorporation of only a few layered silicates, dispersed at the nanometer scale.[9–15] In barrier properties, the layered silicate/polyimide nanocomposite effectively retards the diffusion of water and gas molecules into the polyimide matrix. This is due to an increase in the total diffusion path, since the high-aspect ratio layered silicates are impermeable.[9–11,14,16,17] The nanometer-sized, layered silicates create a similar diffusion barrier for Cu. In this article, the diffusion process, at the interface of Cu/layered silicate-polyimide nanocomposites, is investigated with secondary ion mass spectrometry (SIMS) and transmission electron microscopy (TEM). These techniques provide an assessment of these nanocomposites for use as advanced dielectric materials in microelectronic applications.

EXPERIMENTAL

Fluorinated polyimide (6FDA-ODA) was synthesized by 4,4′-(hexafluoroisopropylidene)-diphathalic anhydride (6FDA) and 4,4′-oxydianiline (ODA) in the present study. Synthetic mica containing layered silicates with chemical composition $NaMg_{2.5}Si_4O_{10}F_2$ was also used. In order to make layered silicates miscible with organic polymers, the layered silicates must become partially organophilic, through an ion exchange step in which the sodium ion in the layer gallery is replaced with an organic molecule containing ammonium ion. This small organic molecule is termed the swelling agent. The swelling agent used in this study is 4-(4-1,1-di[4-(4-aminophenoxy)phenyl]ethylphenoxy)aniline ($3NH_2$) and was synthesized in our laboratory.[13] Detailed procedures for preparing organically modified mica and the synthesis of 6FDA-ODA and $3NH_2$-Mica/6FDA-ODA have been described elsewhere.[12–15] The molecular weights (M_n) of pure 6FDA-ODA and 3 wt % $3NH_2$-Mica/6FDA-ODA were 73,000 and 80,000, respectively, as determined by gel

Correspondence to: K.-H. Wei (khwei@cc.nctu.edu.tw).
Contract grant sponsor: National Science Council; contract grant number: NSC 90-2216-E-009-017.

Journal of Applied Polymer Science, Vol. 92, 1422–1425 (2004)
© 2004 Wiley Periodicals, Inc.

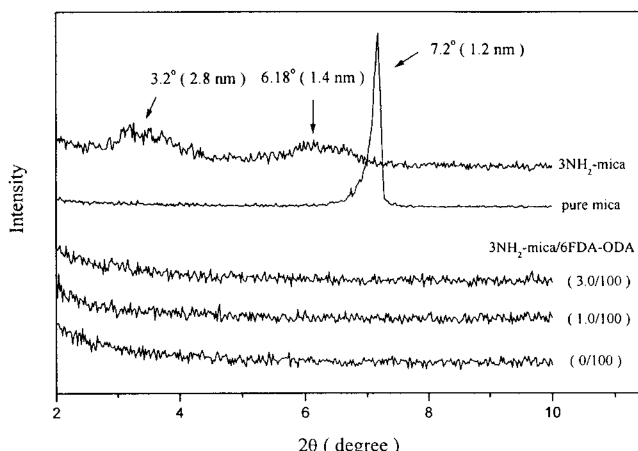

Figure 1 X-ray diffraction curves of the pure mica, $3NH_2$-Mica, and $3NH_2$-Mica/6FDA-ODA films.

permeation chromatography (GPC). A Cu layer was deposited on a polyimide surface through a sputtering process, in which the polyimide film was first heated to 160°C overnight to ensure complete water removal near the surface. Then, 160-nm-thick Cu was deposited on the polyimide films by Ar^+ ion sputtering of a Cu target at room temperature in ultra-high vacuum ($<10^{-9}$ Torr). The purity of the Cu target was 99.99%. Subsequently, two sample structures, Cu/($3NH_2$-Mica/6FDA-ODA) and Cu/($3NH_2$-Mica/6FDA-ODA)/Si, were fabricated for TEM and SIMS analysis. These samples were annealed at 350°C for 2 hours in vacuum before the analysis. Then, the samples were microtomed with a Leica Ultracut Uct into about 100-nm-thick slices. A JEOL JEM-1200EX II TEM was used, with an acceleration voltage of 200 kV. SIMS was performed using a Cameca ims-4f tool, with an etching rate of about 2 nm/sec.

RESULTS AND DISCUSSION

The X-ray diffraction curves of pure mica, $3NH_2$-Mica, and $3NH_2$-Mica/6FDA-ODA are presented in Figure 1. For the pure mica, the strong X-ray diffraction peak at $2\theta = 7.2°$ was caused by the diffraction of the (001) crystal surface of layered silicates, equaling a d-spacing of 1.2 nm. For $3NH_2$-Mica, the weak diffraction peak at $2\theta = 3.2°$ represented a d-spacing of 2.8 nm in silicate layers. Additionally, in Figure 1, no X-ray diffraction peaks at $2\theta = 2$–$10°$ appear in $3NH_2$-Mica/6FDA-ODA films, indicating that the d-spacings of silicate layers in $3NH_2$-Mica were exfoliated.

Figure 2 shows a SIMS depth profile of Cu concentration across the interface between Cu and 6FDA-ODA. In Figure 2(a), in the as-made sample, the Cu and carbon curves represent concentrations of Cu and 6FDA-ODA near the interface, respectively. The intersect between the Cu and the carbon curves can be taken as the center of the interface between the Cu and 6FDA-ODA films. Consequently, the interfacial region can be defined as between 0.16 and 0.20 μm. In Figure 2(b), after being annealed at 350°C for 2 hours in vacuum, the intersect point shifts out of the interfacial region. At secondary ion counts (SCI) equaling 500, the depths of the Cu and carbon curves are 0.64 and 0.10 μm, respectively. These results indicate a large Cu penetration into 6FDA-ODA and some 6FDA-ODA into the Cu layer after annealing.

The Cu concentration profiles at the interface in the cases of annealed 0, 1, and 3 wt % $3NH_2$-Mica/6FDA-ODA nanocomposite films, as analyzed by SIMS, are shown in Figure 3, where log-scale Cu concentration is plotted against the penetration depth. The penetration concentration of Cu into 6FDA-ODA is reduced sharply as the amount of $3NH_2$-Mica in 6FDA-ODA increases. At secondary ion counts equaling 500, the Cu diffusion depths of 6FDA-ODA containing 1 and 3 wt % $3NH_2$-Mica are 0.24 and 0.15 μm, respectively, and are much smaller than that of the pure 6FDA-

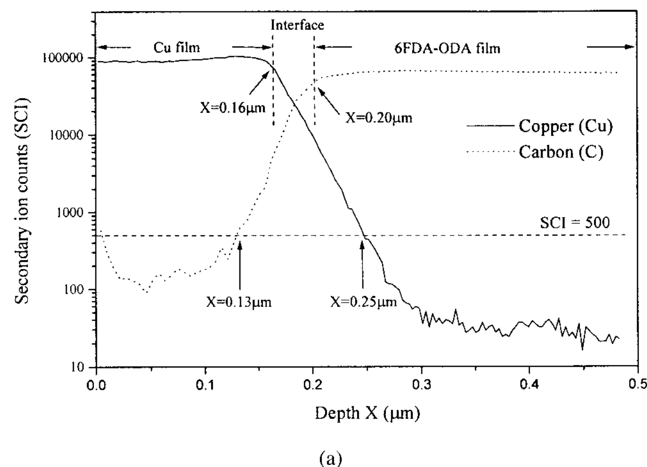

(a)

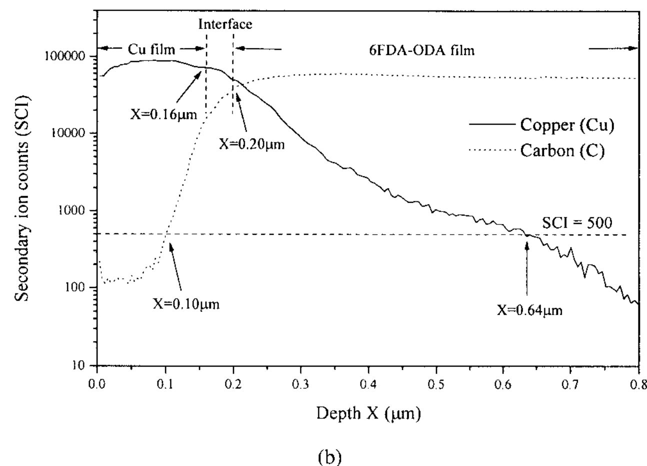

(b)

Figure 2 SIMS Cu concentration depth profiles in 6FDA-ODA: (a) as-made; (b) after annealing at 350°C for 2 hours in vacuum.

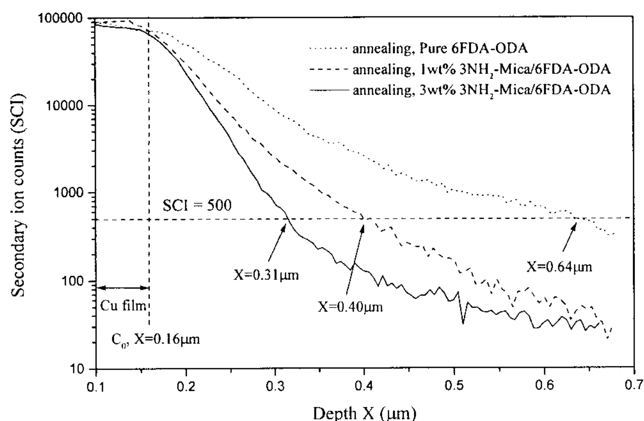

Figure 3 SIMS Cu concentration depth profiles for different compositions of $3NH_2$-Mica/6FDA-ODA nanocomposite films after annealing at 350°C for 2 hours in vacuum.

ODA (0.48 μm). These results indicate that the layered silicates from $3NH_2$-Mica effectively retard the diffusion of Cu into polyimide. In Figure 4, differences in the diffusion characteristics of Cu in pure 6FDA-ODA and 3 wt % $3NH_2$-Mica/6FDA-ODA nanocomposite are clearly demonstrated in TEM micrographs of the cross-sectional area near the interface. In Figure 4(a), the cross section of Cu/6FDA-ODA reveals a black layer, which is the Cu film; the black particles in 6FDA-ODA are Cu particles that have diffused. These Cu particles are distributed uniformly in 6FDA-ODA and the diffusion depth is about 600–700 nm. In Figure 4(b), for Cu/($3NH_2$-Mica/6FDA-ODA), the distribution of Cu particles is confined to the area between the interface and layered silicates (black line), with a diffusion depth of less than 200 nm. This is direct evidence that nanometer-scale layered silicates can prevent Cu from diffusing into 6FDA-ODA near the interface.

For Figure 3, the concentration distribution is described by the complementary error function,[18,19] as shown in eq. (1),

$$C(x,t) = C_0 \times erfc\left(\frac{x}{2\sqrt{Dt}}\right) \quad (1)$$

where C_0 is the constant surface concentration, x is the diffusion depth, t is the diffusion time, and D is the diffusion coefficient. The diffusion coefficients at different depths and with different compositions are given in Table I. The diffusion coefficients have a position-dependence and increase with greater diffusion depths due to a strong surface holdup diffusion mechanism.[18] The strong surface holdup, which is typical of metal diffusion in polymers, can be attributed to strong metal–metal interactions. Most metal atoms form immobile clusters at the surface; therefore the diffusion coefficients are small near the interface. The diffusion coefficients of $3NH_2$-Mica/6FDA-ODA fall sharply with decreasing amounts of $3NH_2$-Mica. For instance, the diffusion coefficients of 6FDA-ODA containing 3 wt % $3NH_2$-Mica decrease by 49% and 72% at 0.44 and 0.09 μm, respectively, from the interface. This result implies that the retardation on Cu diffusion by layered silicates near the interface is more effective than that at other places.

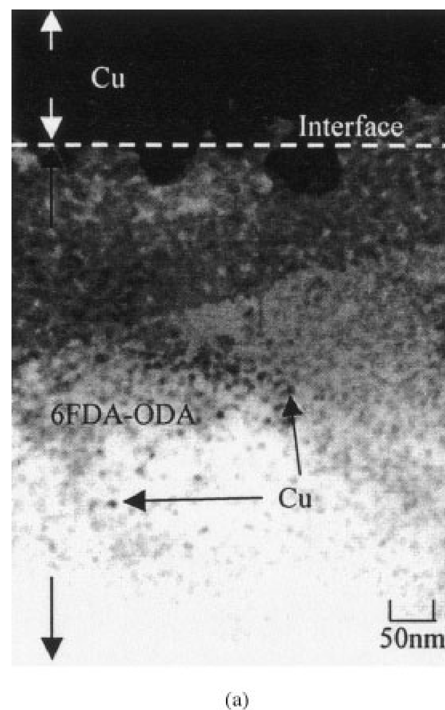

(a)

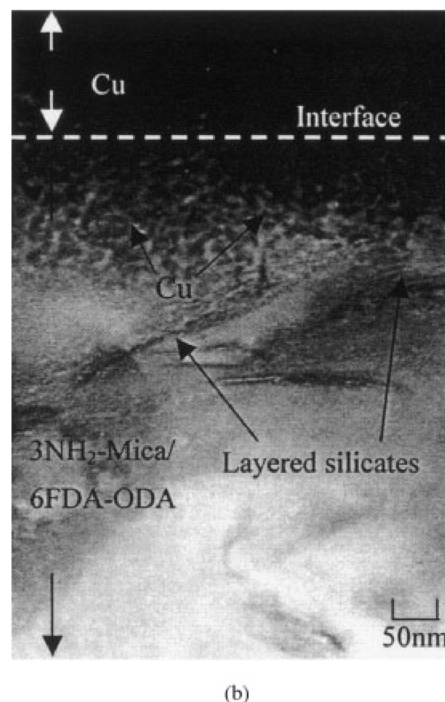

(b)

Figure 4 Transmission electron microscopy micrographs of the cross-sectional view of the interface after annealing: (a) pure 6FDA-ODA; (b) 3 wt % $3NH_2$-Mica/6FDA-ODA.

TABLE I
Diffusion Coefficients of Cu in $3NH_2$-Mica/6FDA-ODA Nanocomposites at Different Depths and Compositions

Contents of $3NH_2$-Mica (wt%)	Diffusion coefficients (cm^2/sec) at different distances from the interface				
	0.09-μm	0.14-μm	0.24-μm	0.34-μm	0.44-μm
0	5.83×10^{-15}	6.65×10^{-15}	9.03×10^{-15}	1.33×10^{-14}	1.97×10^{-14}
1.0	2.20×10^{-15}	3.04×10^{-15}	5.42×10^{-15}	1.10×10^{-14}	1.20×10^{-14}
3.0	1.64×10^{-15}	2.12×10^{-15}	4.14×10^{-15}	7.26×10^{-15}	1.01×10^{-14}

CONCLUSION

In TEM micrographs, these Cu particles are distributed uniformly in 6FDA-ODA and the diffusion depth is about 600–700 nm. For the Cu/($3NH_2$-Mica/6FDA-ODA) case, the distribution of Cu particles is confined to the area between the interface and layered silicates, with a diffusion depth of less than 200 nm. The penetration concentration of Cu into 6FDA-ODA is reduced sharply as the amount of $3NH_2$-Mica in 6FDA-ODA increases. These results indicate the layered silicates from $3NH_2$-Mica effectively retard the diffusion of Cu into polyimide.

References

1. Du, M.; Opila, R. L.; Donnelly, V. M.; Sapjeta, J.; Boone, T. J Appl Phys 1999, 85, 1496.
2. Kim, Y. H.; Kim, J.; Walker, G. F.; Feger, C.; Kowalczyk, S. P. J Adhes Sci Technol 1988, 2, 95.
3. Lee, K. W.; Walker, G. F.; Viehbeck, A. J Adhes Sci Technol 1995, 9, 1125.
4. Kondoh, E.; Nguyen, T. P.; Plachke, D. W.; Carstanjen, H.; Arzt, E. Appl Phys Lett, 70, 1251.
5. Parks, C. C. J Vac Sci Technol A 1997, 15, 1328.
6. Lee, K. W.; Viehbeck, A.; Walker, G. F.; Cohen, S.; Zucco, P.; Chen, R.; Ree, M. J Adhes Sci Technol 1996, 10, 807.
7. Krishnamoorthy, A.; Chanda, K.; Murarka, S. P.; Ramanath, G.; Ryan, J. G. Appl Phys Lett 2001, 78, 2467.
8. Kim, K. J.; Lee, N. E.; Kim, M. C.; Boo, J. H. Thin Solid Films 2001, 398–399, 657.
9. Lan, T.; Kaviratna, P. D.; Pinnavaia, T. J. Chem Mater 1994, 6, 573.
10. Yano, K.; Usuki, A.; Okada, A.; Kurauchi, T.; Kamigaito, O. J Polym Sci, Part A: Polym Chem 1993, 31, 2493.
11. Yano, K.; Usuki, A.; Okada, A. J Polym Sci, Part A: Polym Chem 1997, 35, 2289.
12. Tyan, H. L.; Liu, Y. C.; Wei, K. H. Chem Mater 1999, 11, 1942.
13. Tyan, H. L.; Leu, C. M.; Wei, K. H. Chem Mater 2001, 13, 222.
14. Jiang, L. Y.; Leu, C. M.; Wei, K. H. Adv Mater 2002, 14, 426.
15. Leu, C. M.; Wu, Z. W.; Wei, K. H. Chem Mater 2002, 14, 3016.
16. Giannelis, E. P. Adv Mater 1996, 8, 29.
17. Strawhecker, K. E.; Manias, E. Chem Mater 2000, 12, 2943.
18. Willecke, R.; Faupel, F. Macromolecules 1997, 30, 597.
19. Kim, N. Y.; Yoon, H. S.; Kim, S. Y.; Whang, C. N.; Kim, K. W.; Cho, S. J. J Vac Sci Technol B 1999, 17, 380.20.